Electrochemical and thermodynamic studies of *N*-(phenol-*p*-ylmethylene)-2-amino-5-ethyl-1,3,4-thiadiazole as a corrosion inhibitor complemented with theoretical investigations

H.J. Habeeb,[1] N. Betti,[2] H.S. Sultan,[3] A.A.H. Kadhum,[4] L.M. Shaker[1] and A.A. Al-Amiery[1,5]*

[1]Department of Chemical and Process Engineering, Faculty of Engineering and Build Environment, Universiti Kebangsaan Malaysia, Bangi, Selangor 43600, Malaysia
[2]Materials Engineering Department, University of Technology-Iraq, Baghdad 10001, Iraq
[3]Faculty of Engineering, University Warith Al Anbiya'a, Krbala , Iraq
[4]University of Al-Ameed, Karbala, Iraq
[5]Energy and Renewable Technology Centre, University of Technology, Baghdad, Baghdad 10001, Iraq
**E-mail: dr.ahmed1975@gmail.com*

Abstract

Hydrochloric acid is an important mineral acid that is widely used in a variety of applications, including well acidification, water treatment, chemical cleaning, and acid pickling (HCl). Preventing corrosion of metal buildings has aroused much interest due to the huge financial and safety losses that corrosion has caused in many industries. Mild steel is an important structural material in a variety of industries because it is widely used owing to its low cost and excellent physical and mechanical properties. This study looked at the corrosion inhibitory properties of *N*-(phenol-*p*-ylmethylene)-2-amino-5-ethyl-1,3,4-thiadiazole (PAT) for mild steel in 1 M HCl. The anticorrosion efficacy of PAT as an inhibitor was studied using a variety of electrochemical techniques (electrochemical impedance spectroscopy and potentiodynamic polarization). For the studied inhibitor, the greatest inhibition efficiency was observed at an optimal dose of 0.5 mM. The thermodynamic behavior was studied at various temperatures. As a result, the experiment demonstrated that increasing the temperature reduces inhibitor efficiency and increases the corrosion rate. The experiment discussed the effect of temperature in the range of 30, 40, 50, and 60°C on the corrosion inhibitor and showed that the corrosion rate increased from 7.6 to 630.4 mpy. Furthermore, quantum chemistry calculations using density functional theory (DFT) were used to investigate the relationship between inhibition efficacy and inhibitor molecule structure. All of the calculated results agree with the experimental findings.

Received: December 6, 2021. Published: March 29, 2022 doi: 10.17675/2305-6894-2022-11-1-25

Keywords: *DFT, corrosion inhibitor, thermodynamic, thiadiazole.*

Introduction

When developing organic compounds as corrosion inhibitors, it is important to study factors that affect the anticorrosion efficiency [1, 2]. One of these factors is the solution temperature [3, 4]. The activity of synthetic or natural organic corrosion inhibitors depends on the adsorption rate as well as the ability to cover the alloy surface [5, 6]. Significant factors of absorption that depend on the geometric structures and surface charge of the alloy and the electrolyte have been identified. To replace the H_2O molecule adsorbed on the surface of an alloy, the corrosion inhibitor is adsorbed by the surface immersed in an aqueous phase. In recent years, the electrostatic interaction between inhibitor molecules and mild steel surface was increasingly studied using molecular dynamic simulations as a suitable tool to model such interaction [7, 8]. Corrosive acids are exceedingly applied in manufacturing usage, such as pickling, cleaning and descaling in addition to oil and gas well acidizing [9]. As of result of the universal aggressiveness of corrosive solutions, organic corrosion inhibitors are usually utilized to diminish acid attack on alloys [10]. In continuation of previous investigations [11–21], we studied the effect of temperature on the inhibition efficiency of *N*-(phenol-*p*-ylmethylene)-2-amino-5-ethyl-1,3,4-thiadiazole (PAT) at a concentration of 5 mM in 1 M acidic HCl solution and show the thermodynamic behavior where the efficiency of this compound was improved in the previous article with variation of concentration at a fixed solution temperature and then with variation of solution temperature at a fixed solution concentration.

Experimental details

Synthesis

The structure of the investigated inhibitor *N*-(phenol-*p*-ylmethylene)-2-amino-5-ethyl-1,3,4-thiadiazole is shown in Figure 1.

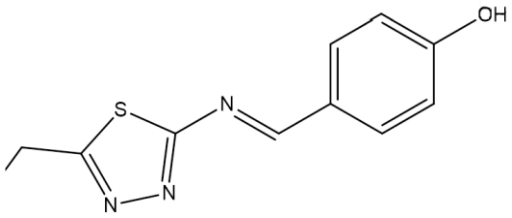

Figure 1. The structure of PAT.

The synthesized inhibitor was studied by spectroscopical techniques, namely FT-IR and ^{1}H NMR, and CHN micro-elemental analysis. In the FT-IR spectrum of the studied inhibitor, the signal at 3396 cm^{-1} represents the phenolic group, the signal at 3077 cm^{-1} corresponds to the aromatic ring, and the signal at 1611 cm^{-1} to C=N. In the ^{1}H NMR spectrum, the triplet signal at 1.540 ppm represents three hydrogen atoms of the methyl group whereas the multiple signals at 3.010 ppm represents hydrogen atoms of the methylene group. The

hydroxyl group signal is observed at 5.830 ppm and that of aromatic hydrogen is at 6.870 to 7.170 ppm.

Temperature effect

Mild steel (MS) was utilized in this investigation. The coupons were cleaned based on the standard methodology reported elsewhere [30].

The adsorption of the inhibitor on mild steel surface was evaluated by electrochemical studies using Gamry equipment and electrochemical techniques: electrochemical impedance spectroscopy (EIS) and potentiodynamic polarization (PD). The temperature was varied in the range from 30 to 60°C to study its effect on the inhibitor efficiency [22, 23]. Figure 2 shows the EIS plots at various temperatures. The largest semi-circle was recorded at 30°C with a low corrosion rate, then with an increase in the temperature, the semi-circles decreased to show that the highest corrosion rate was at 60°C. Figure 3 shows the PD curves at the various temperatures. An increase in temperature results in poorer corrosion inhibition due to weakening of the bonds between corrosion inhibitor molecules and the surface of mild steel samples. E_{corr} shifts to more negative values, from –285 mV to –376 mV…–464 mV. Based on previous investigations, a corrosion inhibitor is classified as anodic or cathodic if the E_{corr} value becomes more than –85 mV [31].

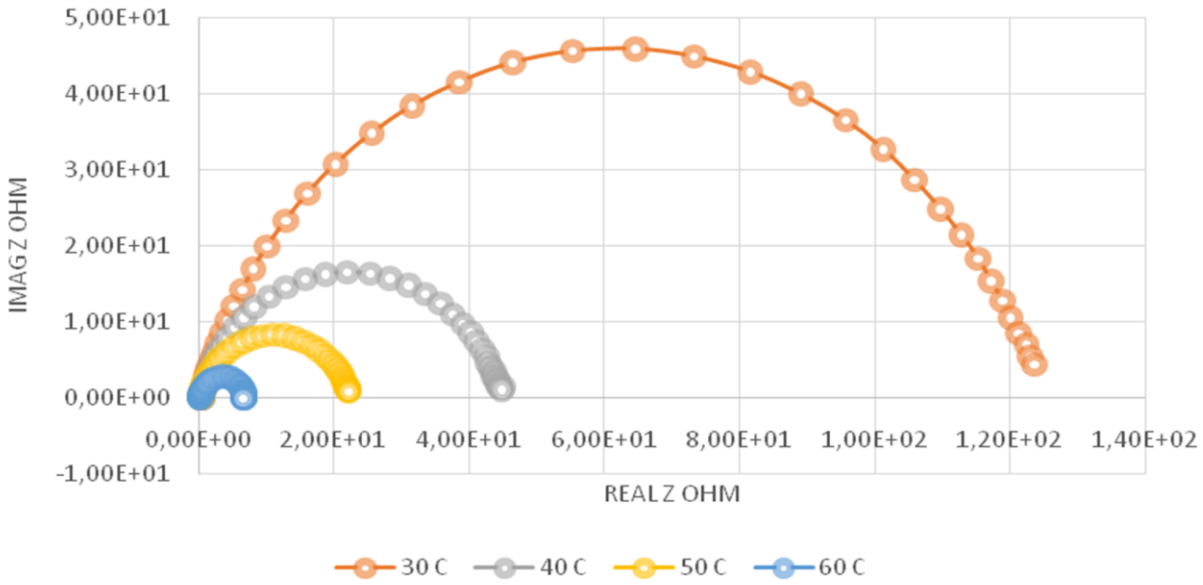

Figure 2. Nyquist Plot of mild steel with PAT inhibitor at various temperatures.

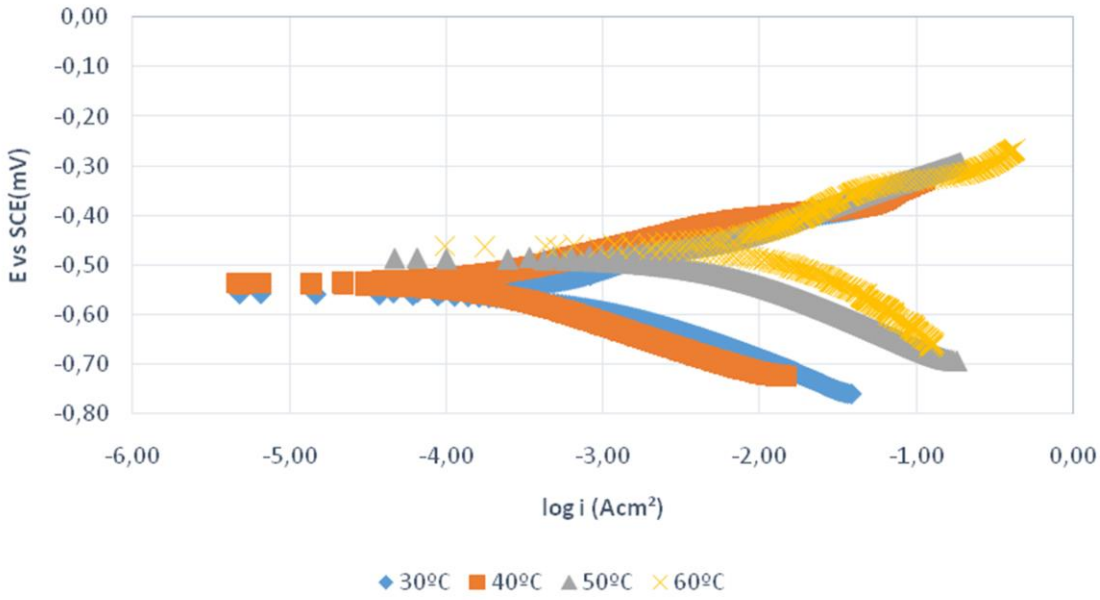

Figure 3. PD curve for mild steel with PAT inhibitor at different temperatures.

Computational studies

Comparison between the $E_{HOMO} - E_{LUMO}$ gaps (energies of highest occupied and lowest unoccupied molecular orbitals) was done using the DFT method, where for the latter the hybrid functional B3LYP was utilized for the studied geometry improvements. The computations were conducted using Gaussian 09, Correction A.02. The ground-state chemical structure improvements were done without symmetry limitations using the 6-311++G(d,p) basis set [32, 33].

Result and Discussion

The investigated inhibitor, namely the PAT compound, was tested by electrochemical techniques (EIS and PD) in 1 M HCl acid solution.

Corrosion inhibitor thermodynamics

The effect of temperature of *N*-(phenol-*p*-ylmethylene)-2-amino-5-ethyl-1,3,4-thiadiazole (PAT) inhibitor was studied in this test and it was found that an increase in the solution temperature led to an increase in the corrosion rate and a decrease in the inhibitor efficiency. The temperature was varied from 30 to 60°C. This variation resulted in a decrease in the inhibitor efficiency form 93% to 35% and an increase in the corrosion rate from 7.601 to 630.4 mpy [24]. The reaction energy or so called activation energy E_a for both the anodic and cathodic reactions in 1 M HCl for different temperatures was calculated using the Arrhenius equation and plotted as in Equation 1 [25, 23].

$$C_r = A\exp\left(\frac{-E_a}{RT}\right) \quad (1)$$

where C_r is the corrosion rate, E_a is the activation energy of the reaction, A is the Arrhenius constant, T is the solution temperature and R is the ideal gas constant. The plot of $\ln(C_r)$ *vs.* $1/T$ values shown in Table 1 and Figure 4 gave a linear relationship with a slope of E_a/R at 0.5 M inhibitor concentration for various temperatures with and without the inhibitor. The activation energy values with and without the PAT inhibitor for this test were 62.35 and 32.95 kJ/mol, respectively.

Table 1. Effect of temperature variation on the corrosion rate.

T	$1/T$	C_r with I	$\ln C_r$ with I	E_a without I	E_a with I	C_r without I	$\ln C_r$ without I
30	0.033	7.6	4.404	32.954	–62.355	5	1.747
40	0.025	76.7	9.424	94.021	–83.14	150	5.440
50	0.020	255	12.033	150.060	–103.925	1000	7.500
60	0.017	630.4	13.998	209.484	–124.71	5000	9.247

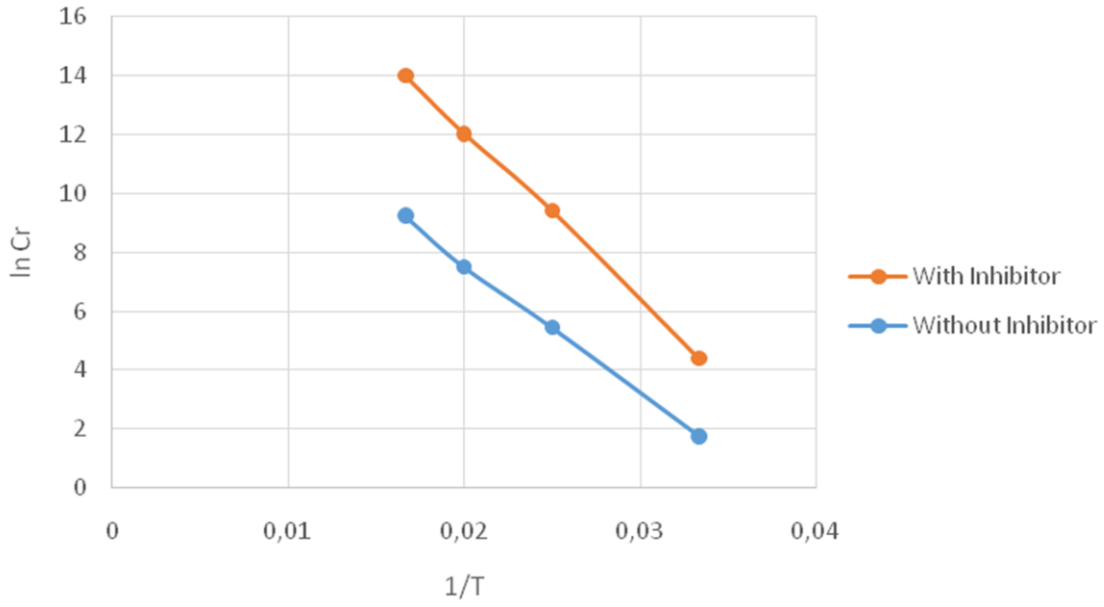

Figure 4. Arrhenius plot for the blank solution and at 0.5 M of the inhibitor in 1 M HCl.

Corrosion inhibitor adsorption isotherm

To better understand the corrosion behavior of mild steel surface, one has to study the isothermal adsorption process in order to find out the effect of temperature on the corrosion rate and the inhibitor efficiency [26]. From the Arrhenius plot it is clear that increasing the

solution temperature leads to an increase in the corrosion rate and thus decrease the inhibitor efficiency [23]. The activation energy in the range less than 20 kJ/mol indicates that the adsorption occurs as physical adsorption [27]. Higher E_a values indicate the adsorption of PAT inhibitor on mild steel surface occurs as chemical adsorption [28].

The Gibbs free energy ΔG_{ads} for this process can be calculated form Equation 2 to determine the adsorption isotherm for the anodic and cathodic reactions.

$$\Delta G_{ads} = -RT\ln(55.5K_{ads}) \quad (2)$$

where R is the ideal gas constant and K_{ads} is the adsorption process equilibrium constant. The ΔG_{ads} values above 20 kJ/mol indicate that the adsorption is chemical adsorption. It was found to be 37.45 kJ/mol, indicating strong interaction between the PAT molecule and the surface of the metal sample in 1 M HCl solution.

The inhibitor performance in the acid solution on mild steel surface can be attributed to adsorption on the metal surface, where its affected the charge density and performance of the bonds between the metal surface and the inhibitor. The molecular structure of this inhibitor is shown in Figure 1. The inhibition effectiveness of PAT relies fundamentally on the nature and structure of the adsorbed layers on the alloy surface.

Our inhibitor comprises an aromatic benzene ring, a heteroaromatic ring and heteroatoms N, O, and S, which have higher electron density that make the inhibitor a good donor and make it form a protective layer on the metal surface where it can form coordination bonds between the mild steel surface and the inhibitor [1, 29].

DFT Investigations

The elucidation of the considerable electronic impact of the studied inhibitor molecules namely PAT with a hydroxyl (–OH) as a strong electron-donating group was investigated by DFT. The phenyl ring in PAT molecule has a hydroxyl group at the *para*-position while this hydroxyl group may move to the *meta*-position (PATa) and *ortho*-position (PATb). For the three molecular positions (*ortho*, *meta* and *para*), the contribution of the hydroxyl group to both the HOMO and LUMO was similar with only small variations, as shown in Figure 5. The geometrical optimization structures of the studied isomers PAT, PATa and PATb are displayed in Figure 5, and the electronic energies are listed in Table 2.

Table 2. Calculated energies, ionization potentials, and electron affinities (eV) for TAP, TAPa and TAPb obtained with rB3LYP/6-31G(d,p).

Molecule	E_{HOMO}	E_{LUMO}	Energy gap	Ionization potential (I)	Electron affinity (A)
PAT	–8.026	–2.190	5.836	8.026	2.190
PATa	–8.022	–2.868	5.154	8.022	2.868
PATb	–8.068	–3.034	5.034	8.068	3.034

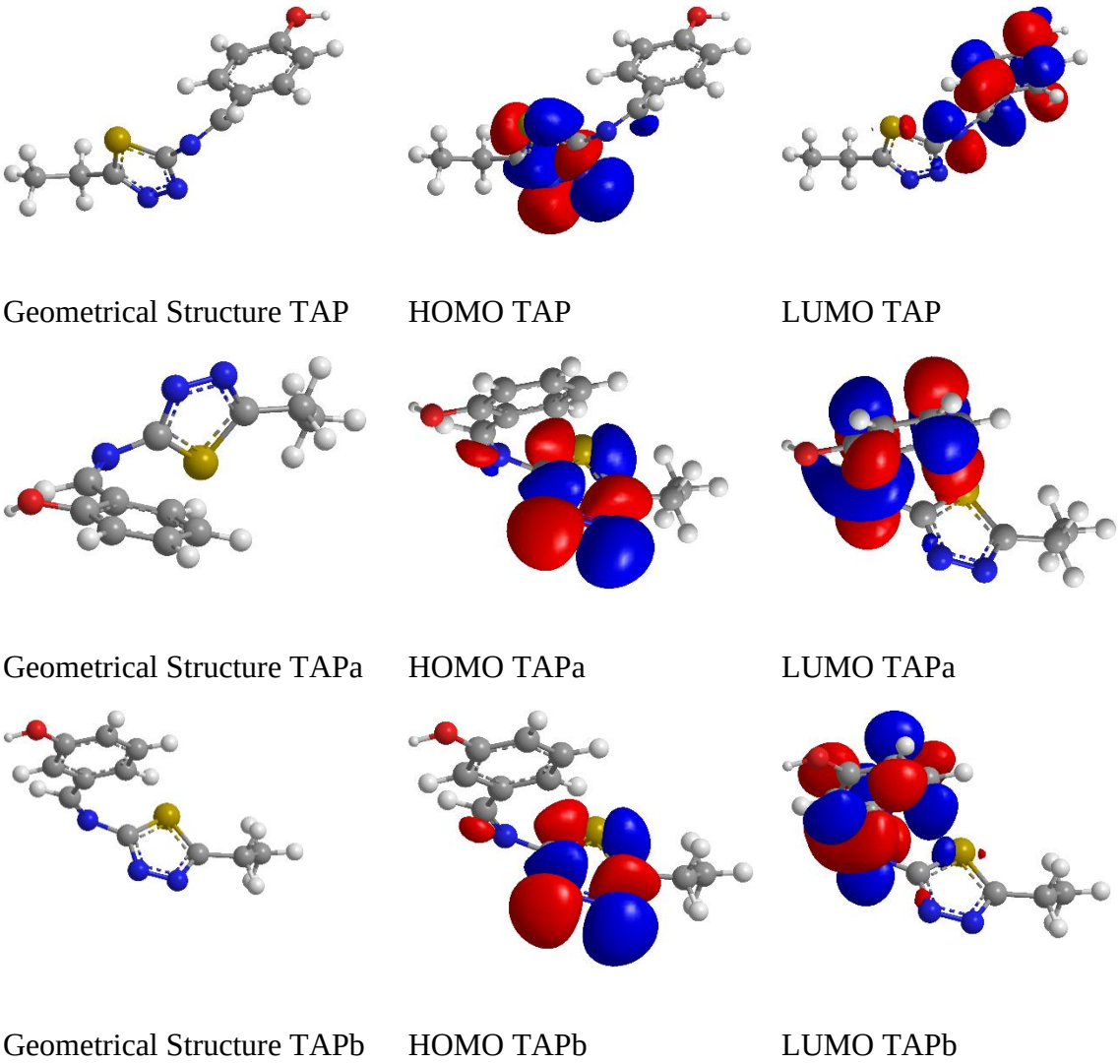

Figure 5. Optimized molecular geometry structures, HOMOs "highest occupied molecular orbitals" and LUMOs "lowest unoccupied molecular orbitals", of PAT, PATa and PATb obtained through rB3LYP/6-31G(d,p).

The (I) and (A) values were calculated based on Koopmans' theorem [34] as follows:

$$I = -E_{\mathrm{HOMO}};\ A = -E_{\mathrm{LUMO}}$$

Vosta *et al*. [35] stated that there is an important correlation between the inhibition efficiency, E_{HOMO}, and E_{LUMO}. Their results showed that the inhibition efficiency increases with a decrease in the ionization potential, as they mentioned that the least firmly bonded electrons in the limit HOMO orbital are those richest in energy. If the ionization of a molecule is somehow favoured, the molecule acts as an electron donor to block the corrosion reaction. Electron affinity analysis has shown effective inhibitors are bad electron acceptors. Substances that are prone to reduction may behave as corrosion stimulators [35].

The ionization potential is the energy required to remove electrons from atoms [36]. The ionization potential reflects the stability of molecules. A high value of ionization potential will indicate a stabile molecule. Although the molecule is stable, when the ionization potential is high, the molecule is excited less.

The approach of Al-Amiery *et al*. [37,38] was utilized to calculate the PAT inhibition efficiency (%) using equations 3–5. The results are displayed in Table 3.

$$I_{\text{add}}\% = \frac{I_{\text{TAB}} - I_{\text{X–TAB}}}{I_{\text{BZ3}}} \cdot 100\% \quad (3)$$

$$Ie_{\text{add}}\% = I_{\text{add}}\% \cdot Ie_{\text{TAB}}\% \quad (4)$$

$$Ie_{\text{theory}}\% = I_{\text{TAB}}\% + Ie_{\text{add}}\% \quad (5)$$

where I_{add}% is the percent variation in the ionization potential of model x-PAT [x-PAT = (PAT) or (PATa) or (PATb)] relative to that of PAT; also Ie_{add}% and Ie_{theory}% are the additional and theoretical inhibition performances, respectively.

Table 3. Inhibition efficiencies (theoretical) for PAT, PATa and PATb.

Compound	**Inhibition efficiency (%)**	
	Theoretical (Ie_{theory})	**Experimental**
PAT	90.82	90
PATa	88.57	–
PATb	82.73	–

These results indicate that transferring the hydroxyl group to a *meta*-position (PATb) decreased the inhibition performance to 82.73%, on the other hand, the inhibition performance for the *ortho*-position for compound PATa became 88.57%. A comparison between PAT and PATa inhibition efficiencies (99.82% *vs*. 88.57%) reveals that this change in the substituent position clearly enhances the inhibition efficiency [39–44].

Functional groups which have non-shared electrons, like the hydroxy group (PAT), provide superior performance if the substituent is arranged at *para*- or *ortho*-positions thus active groups donate electron pairs to the π-system to make a negative charge on *ortho*- or *para*-positions. These positions have superior activity toward the electron-poor electrophile. The maximum electron densities were located at *ortho* and/or *para*-positions.

Conclusion

The thermodynamic part of this paper where the effect of temperature in the range 30, 40, 50 and 60°C on the behavior of *N*-(phenol-*p*-ylmethylene)-2-amino-5-ethyl-1,3,4-thiadiazole (PAT) was studied proved that the adsorption of this compound on the metal

surface occurred as chemical adsorption. The corrosion current (i_{corr}) and corrosion rate are higher when the temperature of the solution increases while the bonds of the corrosion inhibitor molecules with mild steel surface weaken thus allowing the corrosion process to occur more quickly.

Acknowledgement

The authors like to thank Universiti Kebangsaan Malaysia for the support by SUSPRO-YSD as well as by CRIM with grant 2016-020.

References

1. D. Mahmood, A.K. Al-Okbi, M.M. Hanon, K.S. Rida, A.F. Alkaim, A.A. Al-Amiery, A. Kadhum and A.A.H. Kadhum, Carbethoxythiazole corrosion inhibitor: as an experimentally model and DFT theory, *J. Eng. Appl. Sci*., 2018, **13**, no. 11, 3952–3959.
2. A. Kadhim, E.T. Salim, S.M. Fayadh, A.A. Al-Amiery, A.A.H. Kadhum and A. Mohamad, Effect of Multipath Laser Shock Processing on Microhardness, Surface Roughness And Wear Resistance of 2024-T3 Al Alloy, *Sci. World J*., 2014, 490951, 1–6. doi: 10.1155/2014/490951
3. A. Alobaidy, A. Kadhum, S. Al-Baghdadi, A. Al-Amiery, A. Kadhum, E. Yousif and A.B. Mohamad, Eco-friendly corrosion inhibitor: experimental studies on the corrosion inhibition performance of creatinine for mild steel in HCl complemented with quantum chemical calculations, *Int. J. Electrochem. Sci*., 2015, **10**, no. 1, 3961–3972.
4. S. Junaedi, A.A.H. Kadhum, A. Al-Amiery, A.B. Mohamad and M.S. Takriff, Synthesis and characterization of novel corrosion inhibitor derived from oleic acid: 2-Amino-5-Oleyl 1,3,4-Thiadiazol (AOT), *Int. J. Electrochem. Sci*., 2012, **7**, no. 4, 3543–3554.
5. A.Y.I. Rubaye, K.S. Rida, A.Q. Salam and A. Al-Amiery, Acetamidocoumarin as a based eco-friendly corrosion inhibitor, *Int. J. ChemTech Res*., 2016, **9**, no. 11, 39–47.
6. H.J. Habeeb, H.M. Luaibi, T.A. Abdullah, R.M. Dakhil, A.A.H. Kadhum and A.A. Al-Amiery, Case study on thermal impact of novel corrosion inhibitor on mild steel, *Case Stud. Therm. Eng*., 2018, **12**, 64–68. doi: 10.1016/j.csite.2018.03.005
7. S.S. Al-Taweel, K.W.S. Al-Janabi, H.M. Luaibi, A.A. Al-Amiery and T.S. Gaaz, Evaluation and characterization of the symbiotic effect of benzylidene derivative with titanium dioxide nanoparticles on the inhibition of the chemical corrosion of mild steel, *Int. J. Corros. Scale Inhib*., 2019, **8**, no. 4, 1149–1169. doi: 10.17675/2305-6894-2019-8-4-21
8. D.M. Jamil, A.K. Al-Okbi, S.B. Al-Baghdadi, A.A. Al-Amiery, A. Kadhim, T.S. Gaaz, A.A.H. Kadhum and A.B. Mohamad, Experimental and theoretical studies of Schiff bases as corrosion inhibitors, *Chem. Cent. J*., 2018, **12**, no. 7, 1–7. doi: 10.1186/s13065-018-0376-7

9. M.H.O. Ahmed, A.A. Al-Amiery, Y.K. Al-Majedy, A.A.H. Kadhum, A.B. Mohamad and T.S. Gaaz, Synthesis and characterization of a novel organic corrosion inhibitor for mild steel in 1M hydrochloric acid, *Results Phys*., 2018, **8**, 728–733. doi: 10.1016/j.rinp.2017.12.039
10. M.S. Abdulazeez, Z.S. Abdullahe, M.A. Dawood, Z.K. Handel, R.I. Mahmood, S. Osamah, A.H. Kadhum, L.M. Shaker and A.A. Al-Amiery, Corrosion inhibition of low carbon steel in HCl medium using a thiadiazole derivative: weight loss, DFT studies and antibacterial studies, *Int. J. Corros. Scale Inhib*., 2021, **10**, no. 4, 1812–1828. doi: 10.17675/2305-6894-2021-10-4-27
11. A.A. Al-Amiery, A. Kadhim, A. Al-Adili and Z.H. Tawfiq, Limits and developments in ecofriendly corrosion inhibitors of mild steel: a critical review. Part 1: Coumarins, *Int. J. Corros. Scale Inhib*., 2021, **10**, no. 4, 1355–1384. doi: 10.17675/2305-6894-2021-10-4-1
12. M.A. Dawood, Z.M.K. Alasady, M.S. Abdulazeez, D.S. Ahmed, G.M. Sulaiman, A.A.H. Kadhum, L.M. Shaker and A.A. Alamiery, The corrosion inhibition effect of a pyridine derivative for low carbon steel in 1 M HCl Medium: Complemented with antibacterial studies, *Int. J. Corros. Scale Inhib*., 2021, **10**, no. 4, 1766–1782. doi: 10.17675/2305-6894-2021-10-4-25
13. T.A. Salman, D.S. Zinad, S.H. Jaber, M. Shayaa, A. Mahal, M.S. Takriff and A.A. Al-Amiery, Effect of 1,3,4-thiadiazole scafold on the corrosion inhibition of mild steel in acid medium: an experimental and computational study, *J. Bio- Tribo-Corros*., 2019, **5**, no. 48, 1–11. doi: 10.1007/s40735-019-0243-7
14. H.J. Habeeb, H.M. Luaibi, R.M. Dakhil, A.A.H. Kadhum, A.A. Al-Amiery and T.S. Gaaz, Development of new corrosion inhibitor tested on mild steel supported by electrochemical study, *Results Phys*., 2018, **8**, 1260–1267. doi: 10.1016/j.rinp.2018.02.015
15. A. Kadhim, A.K. Al-Okbi, D.M. Jamil, A. Qussay, A.A. Al-Amiery, T.S. Gaas, A.A.H. Kadhum, A.B. Mohamad and M.H. Nassir, Experimental and theoretical studies of benzoxazines corrosion inhibitors, *Results Phys*., 2017, **7**, 4013–4019. doi: 10.1016/j.rinp.2017.10.027
16. A.A. Al-Amiery and L.M. Shaker, Corrosion inhibition of mild steel using novel pyridine derivative in 1 M hydrochloric acid, *Koroze Ochr. Mater*., 2020, **64**, no. 2, 59–64. doi: 10.2478/kom-2020-0009
17. A.A. Al-Amiery, A.A.H. Kadhum, A.H.M. Alobaidy, A.B. Mohamad and P.S. Hoon, Novel corrosion inhibitor for mild steel in HCl, *Materials*, 2014, **7**, no. 2, 662–672. doi: 10.3390/ma7020662
18. A.A. Al-Amiery, A.A.H. Kadhum, A.B. Mohamad and S. Junaedi, A novel hydrazinecarbothioamide as a potential corrosion inhibitor for mild steel in HCl, *Materials*, 2013, **6**, no. 4, 1420–1431. doi: 10.3390/ma6041420

19. A.A. Al-Amiery, A.A.H. Kadhum, A. Kadihum, A.B. Mohamad, C.K. How and S. Junaedi, Inhibition of mild steel corrosion in sulfuric acid solution by new Schiff base, *Materials*, 2014, **7**, no. 2, 787–804. doi: 10.3390/ma7020787
20. A.B. Mohamad, A.A.H. Kadhum, A.A. Al-Amiery, L.C. Ying and A.Y. Musa, Synergistic of a coumarin derivative with potassium iodide on the corrosion inhibition of aluminum alloy in 1.0 M H_2SO_4, *Met. Mater. Int*., 2014, **20**, 459–467. doi: 10.1007/s12540-014-3008-3
21. A.A. Al-Amiery, A.A.H. Kadhum, A.B. Mohamad, A.Y. Musa and C.J. Li, Electrochemical study on newly synthesized chlorocurcumin as an inhibitor for mild steel corrosion in hydrochloric acid, *Materials*, 2013, **6**, no. 12, 5466–5477. doi: 10.3390/ma6125466
22. A.A. Abu-Hashem, Synthesis and antimicrobial activity of new 1,2,4-triazole, 1,3,4-oxadiazole, 1,3,4-thiadiazole, thiopyrane, thiazolidinone, and azepine derivatives, *J. Heterocycl. Chem*., 2021, **58**, 74–92. doi: 10.1002/jhet.4149
23. A. Kadhim, A.A. Al-Amiery, R. Alazawi, M.K.S. Al-Ghezi and R.H. Abass, Corrosion inhibitors. A review, *Int. J. Corros. Scale Inhib*., 2021, **10**, no. 1, 54–67. doi: 10.17675/2305-6894-2021-10-1-3
24. M. Hanoon, D.S. Zinad, A.M. Resen and A.A. Al-Amiery, Gravimetrical and surface morphology studies of corrosion inhibition effects of a 4-aminoantipyrine derivative on mild steel in a corrosive solution, *Int. J. Corros. Scale Inhib*., 2020, **9**, no. 3, 953–966. doi: 10.17675/2305-6894-2020-9-3-10
25. E. Yousif, Y.F. Win, A.H. Al-Hamadani, A. Al-Amiery, A.A.H. Kadhum and A.B. Mohamad, Furosemide as an environmental-friendly inhibitor of corrosion of zinc metal in acid medium: Experimental and theoretical studies, *Int. J. Electrochem. Sci*., 2015, **10**, 1708–1718.
26. S.B. Al-Baghdadi, F.T.M. Noori, W.K. Ahmed and A.A. Al-Amiery, Thiadiazole as a potential corrosion inhibitor for mild steel in 1 M HCl, *J. Adv. Electrochem*., 2016, **2**, 67–69.
27. K.F. Al-Azawi, I.M. Mohammed, S.B. Al-Baghdadi, T.A. Salman, H.A. Issa, A.A. Al-Amiery, T.S. Gaaz and A.A.H. Kadhum, Experimental and quantum chemical simulations on the corrosion inhibition of mild steel by 3-((5-(3,5-dinitrophenyl)-1,3,4-thiadiazol-2-yl)imino)indolin-2-one, *Results Phys*., 2018, **9**, 278–283. doi: 10.1016/j.rinp.2018.02.055
28. S. Junaedi, A. Al-Amiery, A. Kadihum, A.H. Kadhum and A. Mohamad, Inhibition Effects of a Synthesized Novel 4-Aminoantipyrine Derivative on the Corrosion of Mild Steel in Hydrochloric Acid Solution together with Quantum Chemical Studies, *Int. J. Mol. Sci*., 2013, **14**, 11915–11928. doi: 10.3390/ijms140611915

29. M.H.O. Ahmed, A.A. Al-Amiery, Y.K. Al-Majedy, A.A.H. Kadhum, A.B. Mohamad and T.S. Gaaz, Synthesis and characterization of a novel organic corrosion inhibitor for mild steel in 1 M hydrochloric acid, *Results Phys*., 2018, **8**, 728–733. doi: 10.1016/j.rinp.2017.12.039
30. ASTM G-31-72, Standard recommended practice for the laboratory immersion corrosion testing of metals, ASTM, Philaldelphia, PA, 1990, 401.
31. A.A. Al-Amiery, F.A.B. Kassim, A.A.H. Kadhum and A.B. Mohamad, Synthesis and characterization of a novel eco-friendly corrosion inhibition for mild steel in 1 M hydrochloric acid, *Sci. Rep*., 2016, **6**, 19890. doi: 10.1038/srep19890
32. M.J. Frisch, G.W. Trucks, H.B. Schlegel, G.E. Scuseria, M.A. Robb, J.R. Cheeseman, G. Scalmani, V. Barone, G.A. Petersson, H. Nakatsuji, X. Li, M. Caricato, A. Marenich, J. Bloino, B.G. Janesko, R. Gomperts, B. Mennucci, H.P. Hratchian, J.V. Ortiz, A.F. Izmaylov, J.L. Sonnenberg, D. Williams-Young, F. Ding, F. Lipparini, F. Egidi, J. Goings, B. Peng, A. Petrone, T. Henderson, D. Ranasinghe, V.G. Zakrzewski, J. Gao, N. Rega, G. Zheng, W. Liang, M. Hada, M. Ehara, K. Toyota, R. Fukuda, J. Hasegawa, M. Ishida, T. Nakajima, Y. Honda, O. Kitao, H. Nakai, T. Vreven, K. Throssell, J.A. Montgomery, Jr., J.E. Peralta, F. Ogliaro, M. Bearpark, J.J. Heyd, E. Brothers, K.N. Kudin, V.N. Staroverov, T. Keith, R. Kobayashi, J. Normand, K. Raghavachari, A. Rendell, J.C. Burant, S.S. Iyengar, J. Tomasi, M. Cossi, J.M. Millam, M. Klene, C. Adamo, R. Cammi, J.W. Ochterski, R.L. Martin, K. Morokuma, O. Farkas, J.B. Foresman and D.J. Fox, Gaussian 09, Revision A.02, Gaussian, Inc., Wallingford CT, 2016.
33. N. Kovačević and A. Kokalj, Analysis of molecular electronic structure of imidazole- and benzimidazole-based inhibitors: a simple recipe for qualitative estimation of chemical hardness, *Corros. Sci*., **53**, no. 3, 2011, 909–921. doi: 10.1016/j.corsci.2010.11.016
34. T. Koopmans, Über die Zuordnung von Wellenfunktionen und Eigenwerten zu den Einzelnen Elektronen Eines Atoms, *Physica*, 1933, **1**, 104–113 (in German). doi: 10.1016/S0031-8914(34)90011-2
35. J. Vosta and J. Eliasek, Study on corrosion inhibition from aspect of quantum chemistry, *Corros. Sci*., 1971, **11**, 223–229. doi: 10.1016/S0010-938X(71)80137-3
36. J.D. Talati and R.M. Modi, O-Substituted Phenols as Corrosion Inhibitors for Aluminium-Copper Alloy in Sodium Hydroxide, *Br. Corros. J*., 1977, **12**, 180–184. doi: 10.1179/bcj.1977.12.3.180
37. H.R. Obayes, G.H. Alwan, A.H.MJ. Alobaidy, A.A. Al-Amiery, A.A.H. Kadhum and A.B. Mohamad, Quantum chemical assessment of benzimidazole derivatives as corrosion inhibitors, *Chem. Cent. J*., 2014, **8**, no. 21, 1–8. doi: 10.1186/1752-153X-8-21

38. H.R. Obayes, A.A. Al-Amiery, G.H. Alwan, T.A. Abdullah, A.A.H. Kadhum and A.B. Mohamad, Sulphonamides as corrosion inhibitor: experimental and DFT studies, *J. Mol. Struct*., 2017, **1138**, 27–34. doi: 10.1016/j.molstruc.2017.02.100
39. A.A.H. Kadhum, A.B. Mohamad, L.A. Hammed, A.A. Al-Amiery, N.H. San and A.Y. Musa, Inhibition of mild steel corrosion in hydrochloric acid solution by new coumarin, *Materials*, 2014, **7**, no. 6, 4335–4348. doi: 10.3390/ma7064335
40. K. Al-Azawi, S. Al-Baghdadi, A. Mohamed, A.A. Al-Amiery, T.K. Abed, S.A. Mohammed, A.H. Kadhum and A. Mohamad, Synthesis, inhibition effects and quantum chemical studies of a novel coumarin derivative on the corrosion of mild steel in a hydrochloric acid solution, *Chem. Cent. J*., 2016, **10**, no. 23. doi: 10.1186/s13065-016-0170-3
41. T.A. Salman, Q.A. Jawad, M.A.M. Hussain, A.A. Al-Amiery, L.M. Shaker, A.A.H. Kadhum, M.S. Takriff and R.R. Hussain, New environmental friendly corrosion inhibitor of mild steel in hydrochloric acid solution: Adsorption and thermal studies, *Cogent Eng*., 2020, **7**, no. 1, 1–17. doi: 10.1080/23311916.2020.1826077
42. A.A. Al-Amiery, Y.K. Al-Majedy, A.A.H. Kadhum and A.B. Mohamad, New coumarin derivative as an eco-friendly inhibitor of corrosion of mild steel in acid medium, *Molecules*, 2015, **20**, no. 1, 366–383. doi: 10.3390/molecules20010366
43. F.G. Hashim, T.A. Salman, S.B. Al-Baghdadi, T. Gaaz and A.A. Al-Amiery, Inhibition Effect of Hydrazine-Derived Coumarin on a Mild Steel Surface in Hydrochloric acid, *Tribologia*, 2020, **37**, no. 3–4, 45–53. doi: 10.30678/fjt.95510
44. A. Al-Amiery, New Corrosion Inhibitor Derived from Coumarin, *Preprints*, 2017, 2017080021. doi: 10.20944/preprints201708.0021.v1

♦ ♦ ♦